3D-printed immersion micro optics

Marco Wende, Kathrin Doth, Michael Heymann, and Andrea Toulouse*

Cite this article as: Marco Wende, *et.al*. A Universal 3D-printed immersion micro optics. *Light: Advanced Manufacturing* accepted article preview 24 February 2025; doi: 10.37188/lam.2025.019

Received 19 June 2024; revised 17 January 2025; accepted 18 January 2025; Accepted article preview online 24 February 2025

ACCEPTED ARTICLE PREVIEW
https://doi.org/10.37188/lam.2025.019

Letter Open Access

3D-printed immersion micro optics

Marco Wende[1,2], Kathrin Doth[1,2], Michael Heymann[3] and Andrea Toulouse[1,2,*]

Abstract

Femtosecond 3D-printing offers tantalizing avenues for miniaturization and integration of micro optical systems. Available photoresists, however, restrain their utility in liquid immersion, especially in media with refractive indices larger than n = 1.33, such as glues or biomedical fluids. We present monolithic 3D-printed immersion optics, equipped with compact microfluidic sealing to protect the micro optical device from intrusion of liquid immersion media. We experimentally demonstrate diffraction limited performance in water, silicone-, and immersion oil, for a tailored aspherical-spherical doublet with a numerical aperture of NA = 0.625 and a footprint as small as a single mode optical fiber. Such compact monolithic immersion micro optics yield high potential to advance miniaturization for *in situ* biomedical sensing and robust coupling between fibers and photonic integrated circuits.

Keywords: Femtosecond 3D-printing, Micro optics, Liquid immersion, Microfluidics, Biomedical optics, Photonic integrated circuits

Miniaturization can advance cutting edge optical applications in liquid environments[1,2] by reducing system size, reagent consumption and hence overall system cost[3-5]. Available off-the-shelf optical components, however, such as macroscopic immersion objective lenses (Fig. 1a), are too expensive for single-use measurements and too large for non-destructive *in situ* medical diagnostics inside of small, confined organ cavities. 3D-printed micro optics using femtosecond 3D-printing[6] have been emerging as a suitable alternative. They combine high optical performance with a compact footprint on the order of hundreds of microns[7,8], which is ideal for fiber tip applications[9].

So far, 3D-printed micro optics remained mostly limited to gaseous or evacuated environments, or for solid immersion[9]. Many *in situ* applications, however, would benefit from a practical approach that enables 3D-printed micro optics that are viable for immersion into liquids.

In the biomedical context, successful lab-on-a-tip miniaturization requires immersion optics for illumination and to probe light that carries information about a liquid sample[10]. Raman-spectroscopy for instance excels in label-free identification of cells[11] for disease and tissue diagnostics[12] *in vitro* and *in vivo*[12,13]. Similarly, miniaturized fluorescence correlation spectroscopy may enable minimal invasive *in situ* analyses[14] of dynamic biomolecular properties like diffusion rates, viscosity, binding constants or concentration changes[15] inside of confined patient tissue and small blood vessels (Fig. 1b).

Photonic integrated circuits (PIC) and quantum dot applications encourage compact and stable coupling to optical fibers[16]. 3D-printed photonic wire bonds enable miniaturized and efficient chip-to-chip- and off-chip coupling for PICs[17,18], but their *in situ* manufacturing requires extensive pre-alignment. Alternatively, lensed fibers, grating couplers[19], tapered edge couplers[20], and 3D-printed micro optics[21,22] may provide compact coupling, but they are unstable due to free-space operation. More robust connections were pursued by 3D-printing of an alignment

Correspondence: andrea.toulouse@ito.uni-stuttgart.de
[1]Institute of Applied Optics (ITO), University of Stuttgart, Pfaffenwaldring 9, 70569 Stuttgart, Germany
[2]Research Center SCoPE, University of Stuttgart, Pfaffenwaldring 57, 70569 Stuttgart, Germany
Full list of author information is available at the end of the article.

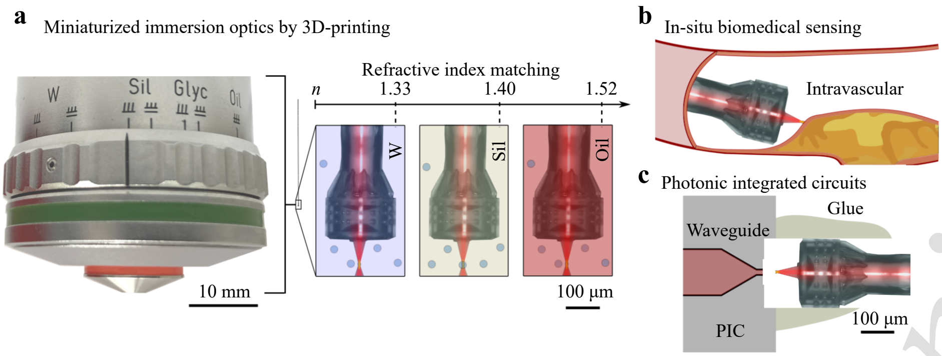

Fig. 1 3D-printed immersion micro optics are highly sought after for *in situ* applications. **a** State-of-the-art macroscopic immersion objective lenses are about 100× larger than 3D-printed micro optics. The flexible 3D-printing approach enables swift design adaptation to match the RI of different immersion media. **b** Compact immersion optics enable applications in confined cavities, e.g. spectroscopy in small arteries. **c** They could also provide stable coupling between fibers and photonic integrated circuits by immersion into glue, active alignment, and subsequent fixing.

chuck directly onto a quantum dot to insert and glue an optical fiber[23,24]. Positioning such a bulky chuck in respect to the quantum emitter, however, was delicate and required extra markers. Immersion micro optics could simplify this process, as glue could be cured in the gaps between micro optical systems and photonic integrated circuits after coupling their modes (Fig. 1c).

An optical surface's ability to refract transmitted light depends on the refractive index (RI)-difference across the interface. Available photoresists for 3D-printing of micro optics ($n \approx 1.5$) are well suited for application in air ($n \approx 1$), but resemble the RI of liquid immersion media ($n \geq 1.33$) very closely. To achieve suitable focusing power, an immersed lens hence requires an extremely strong surface curvature, impractical for femtosecond 3D-printing. Diffractive optical elements (DOEs)[25-27] and metalenses[28,29] offer to circumvent this problem. Compared to the use in air, however, those devices require higher aspect ratios in immersion. This complicates manufacturing, exacerbates shadowing effects and reduces diffraction efficiency, especially when a high numerical aperture (NA) is desired[30].

Engineering a high-RI photoresist to increase the RI-contrast between the lens material and the immersion medium offers another approach towards high performance 3D-printed immersion micro optics. To estimate the required RI, a spherical surface with a constant curvature could be considered: For the same paraxial refractive power as in air ($n \approx 1$), immersion of the surface into water ($n = 1.33$) requires raising the lens material's RI from $n = 1.5$ to at least $n = 2$[42]. Commercial resists such as SU-8, IP-S, IP-Dip, and IP-n162, or widely used custom resists such as SZ2080™[43] have RIs well below this ideal threshold for immersion (Table 1). Doping or admixing nanoparticles can increase the resulting material's RI up to $n \approx 1.9$. Higher volume fractions, however, quickly cause fatal absorption and scattering artifacts. Thus, this approach's feasibility is limited to the engineering of photoresists with $n < 2$, which is too low even for cases with low-RI immersion media such as deionized water ($n = 1.33$).

Table 1 Available photoresists for femtosecond 3D-printing of micro optics fail to provide sufficiently high-RIs to enable refractive high-NA systems in liquid immersion.

Photoresist	n	Availability and comments
SZ2080™	1.51	FORTH, Heraklion, Greece[32], hybrid sol-gel
SU-8	1.58	Kayaku AM, Westborough, Massachussets, USA[33], epoxy
Ge-doped silicate	1.58	Custom[34], doped glass, transparent
IP-S, IP-Dip, IP-n162	1.51, 1.54, 1.62	Nanoscribe GmbH, Eggen-stein-Leopoldshausen, Germany[35,36], acrylic
Proprietary matrix + ZnO_2	≈ 1.7	Custom[37], polymer + nanoparticles, transparent
Custom matrix + TiO_2/Au	≈ 1.9	Custom[38-41], polymer + nanoparticles, low transparency

Practical application for 3D-printed micro optics favors commercial photoresists with a good knowledge of critical material properties, including surface roughness[44], mechanical and physical behavior[45-47], and biocompatibility profiles[48]. As a consequence, important routine practices like iterative surface shape correction to converge the fabricated lens' surface to the designed shape[49,50] have been established for commercial photoresists. Experimental photoresists on the other hand typically lack comparable process knowledge and optimization.

Our 3D-printed immersion micro optical systems (3D-PRIMOPS) achieve high refractive power by maintaining an air-photoresist interface on internal optical surfaces via a microfluidic sealing technique. To the best of our knowledge, refractive 3D-printed liquid immersion optics either have been shielded with a protective sheath[51,52] or a bulky chuck[23,24] in a post fabrication assembly step. The required tolerances increase the systems' mechanical footprint and make them susceptible to misalignment – limitations, that we avoid by combining monolithic manufacturing with a subsequent microfluidic self-sealing step to realize a protective encapsulation. In experiment, our manufactured 3D-PRIMOPS' achieve diffraction limited performance with NA = 0.625, immersed in media ranging from water (n = 1.33) to oil (n = 1.52).

In a first step, ray optical simulations confirm that a refractive lens may achieve high refractive power and diffraction limited performance in air (Fig. 2a, case 1), but fails to focus incident rays upon immersion into water with n = 1.33 (case 2). Even if we bend the immersed lens far beyond the limit of measurement- and thus verifiable manufacturing capabilities (see Methods: Ray tracing and wave optical simulation), its refractive power remains insufficient to create a tight focus (case 3). We conclude that for powerful optical performance, we must avert immediate contact between lens and immersion medium by fabricating a cover structure for protective shielding (case 4) together with the lens, ideally as a single monolith.

While a cylindrical wall would geometrically describe a suitable 3D-encapsulation around the optical system (Fig. 2b), such an airtight structure would entrap uncured photoresist during manufacturing, failing to create an air-filled void. Therefore, we integrate microfluidic channels and vias into the encapsulating wall (Fig. 2c), akin to a process for creating opaque apertures[53]. This facilitates solvation of entrapped resist during development to obtain an air-filled cavity. To prevent intrusion of immersion media through the same vias, we exploit the capillary effect to draw an UV-curable, viscous liquid into the microfluidic channels. Subsequent UV-curing seals all vias permanently.

Adopting this encapsulation strategy, we create a ray optical design of a 3D-PRIMOPS for point illumination, well suited for applications in spectroscopy or integrated fiber coupling. We aim for tight (NA = 0.625) and diffraction limited focusing into a silicone oil (n = 1.4) immersion medium (Fig. 3a). Behind the single mode fiber (SMF), a 650 µm long coreless fused silica fiber (CFSF), spliced at the facet of the SMF for mode expansion, and a subsequent 3D-printed doublet constitute the optical system.

The 3D-printed doublet comprises four interfaces (S1-S4, Fig. 3a). S1 and S2 build the 3D-PRIMOPS' wall facing the CFSF, followed by an air-filled cavity, and behind that, S3 and S4 constitute the wall facing the immersion medium. All these surfaces exert both optical and mechanical functionality to achieve focusing and encapsulation in an assembly-free design. Because of the minute RI-contrast at both surfaces, S1 and S4 barely affect the optical performance. For robust adhesion to the optical

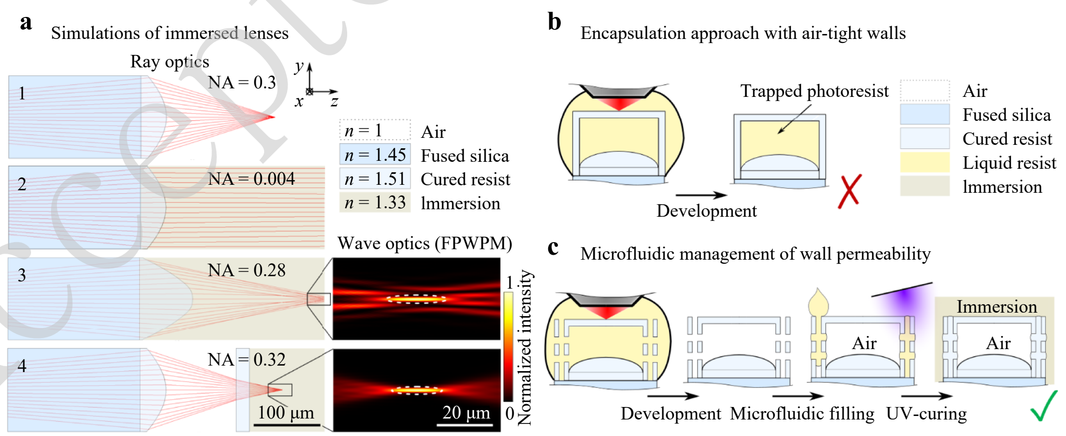

Fig. 2 Our proposed air-tight encapsulation strategy provides micro optics for tight focusing in liquid immersion. **a** Ray optical simulation of light focusing by a 3D-printed lens. While capable of tight and diffraction limited focusing in air (case 1), immersion into water reduces the refractive power of the lens (case 2), preventing tight focusing despite re-optimization (case 3). Encapsulation prohibits intrusion of the immersion medium and preserves the optical system's refractive power, enabling a lens with tight focusing capability (case 4). The white outlines indicate diffraction limited performance at the respective NA in wave optical simulations (Fast Polarized Wave Propagation Method, FPWPM)[31]. **b** Cylindric walls for encapsulation prohibit rinsing uncured photoresist from the capsule's interior after the femtosecond 3D-printing process. **c** Microfluidic channels and vias facilitate creation of air-filled cavities. After loading by capillary action, the resin is cured by UV-light to permanently seal the vias.

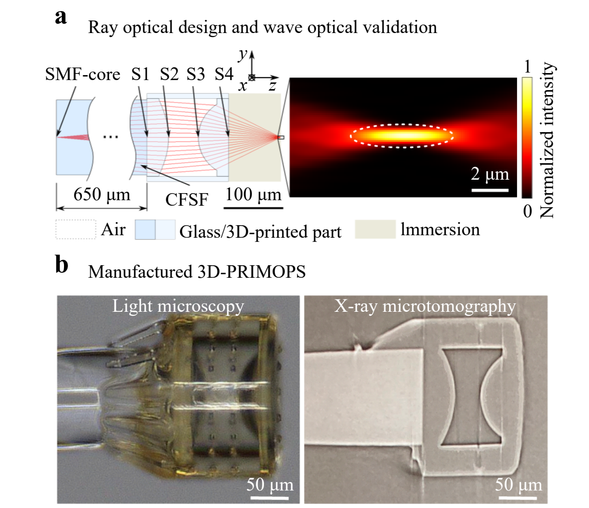

Fig. 3 a Ray optical design of a point illumination 3D-printed immersion micro optical system (3D-PRIMOPS). Four surfaces, S1-S4, constitute the 3D-printed part. A vector wave optical simulation of the 3D-PRIMOPS predicts diffraction limited focusing, outlined by the white dashed line. CFSF: coreless fused silica fiber. **b** Light microscopy- and X-ray microtomography images of a manufactured, encapsulated 3D-PRIMOPS, clearly show the air-filled cavity and the seamless encapsulation.

fiber, we keep S1 flat, and to ensure robust wetting of S4 with the immersion media in this proof-of-concept work, we likewise keep S4 flat. The inner surfaces S2 and S3 exhibit high refractive power due to the large RI-contrast provided by the protective shielding. We therefore use these two surfaces to optimize a high-NA system with moderate angles of incidence on all surfaces, achieving a relaxed optical design. Especially noteworthy in our monolithic approach, S3 contributes to the optical performance positively, whereas in assembled approaches, this inner surface of the capsule usually causes considerable aberrations that require correction[52]. This avoids compromising tolerances and ensures high optical quality as well as robust manufacturing.

Since the small diameter (≈ 125 µm) of the optical system could cause disturbing diffraction effects, we perform a wave optical simulation for validation[31] (Fig. 3a). The simulation confirms diffraction limited focusing for the ray tracing derived 3D-PRIMOPS.

Likewise, we optimize two more 3D-PRIMOPS' adjusted for water ($n = 1.33$) and oil ($n = 1.52$) immersion, to account for a broader range of immersion media. A separate 3D-PRIMOPS has to be manufactured for each distinct immersion medium. Since femtosecond 3D-printing allows for rapid manufacturing of individual surface shapes, the additional effort to adjust the design to different immersion media is minute.

For experimental proof, we manufacture the three 3D-PRIMOPS' designed for water-, silicone-, and oil immersion with a femtosecond 3D-printer and carry out the microfluidic sealing process as outlined above (Fig. 2c). The total probe diameter at the fiber tip is as low as 205 µm. Light microscopy- and X-ray microtomography[54] images show the tightly sealed, air-filled cavity of the 3D-PRIMOPS (Fig. 3b). In experiment, we quantify the point spread function (PSF) of our manufactured 3D-PRIMOPS' (Fig. 4a) and observe diffraction limited focusing for all three 3D-PRIMOPS' (Fig. 4b).

Our results pave the way for manufacturing of complex refractive 3D-printed immersion micro optics with high optical performance and minimal mechanical footprint. The current optical design requires an array of 3D-printed lenses to mimic an immersion correction collar's functionality (Fig. 1a); future optical designs, that are invariant to RI-changes of the immersion medium[55], could provide similar functionality within one single optical device to further minimize the fabrication time and the mechanical footprint. Moreover, the presented microfluidic shielding may promote various complex immersion systems for illumination, imaging, and light collection, such as stacked 3D-printed dielectric metasurfaces[28] or high-NA hybrid microlenses for holographic optical trapping[56]. We anticipate broad applicability in miniaturized analytical devices for biomedical research, keyhole access medical endoscopy, and photonic integrated circuit coupling.

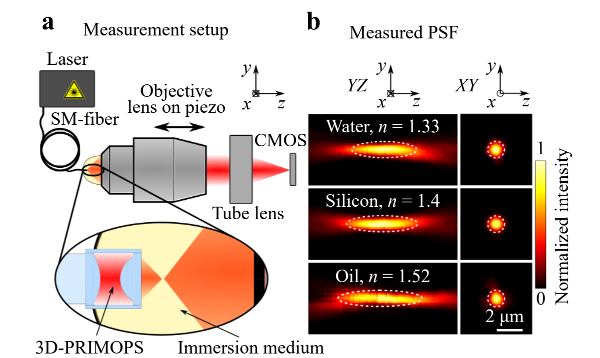

Fig. 4 a Setup for PSF measurement of 3D-PRIMOPS' in immersion. Light is coupled into the SMF with the 3D-PRIMOPS, which is immersed directly. A microscope setup images the 3D-PRIMOPS' focal area onto a CMOS sensor. Volume stacks of the intensity in the 3D-PRIMOPS' focal area are acquired using a piezo stepper for z-scanning. **b** Measured PSFs for water-, silicone- and oil immersion. The white outlines indicate diffraction limited performance at NA = 0.625.

Methods

Ray tracing and wave optical simulation

Ray tracing simulations were performed in Zemax OpticStudio (Ansys, Canonsburg, Pennsylvania, USA). Details on the materials are listed in the manufacturing section. A single mode fiber (SMF) was approximated as a point source, emitting light with $\lambda = 780$ nm and NA = 0.13 into a 650 µm long coreless fused silica fiber (CFSF) with n = 1.458, that provides mode expansion. An even aspheric singlet (Fig. 2) or aspheric-spheric doublet (Fig. 3) lens, made from IP-S with n = 1.505[36], was added to focus this expanded beam into a diffraction limited spot in alternating immersion media, including air (n = 1), water (n = 1.33), silicone oil (n = 1.4) or high-refractive-index (RI) immersion oil (n = 1.52). Due to constant exposure during printing and post UV-treatment, we consider a homogeneous RI for the IP-S material and neglect exposure dependent RI-variation. The lens's surface normal in respect to the optical axis was limited to 45°, according to the experimentally identified limiting surface steepness for confocal surface metrology during iterative surface shape correction[49,50]. The 3D-PRIMOPS (Fig. 2a, case 4) included a 105 µm long cavity (n = 1) behind the lens, followed by a 20 µm thick, flat cover (IP-S, n = 1.505) to shield against silicone immersion. The final 3D-PRIMOPS design (Fig. 3a) used a doublet (IP-S, n = 1.505) behind the CFSF with four surfaces (S1-S4). S1 and S4 are flat, S2 is an asphere, S3 is a sphere. Supplementary file 1 contains the structural data of the initial optical design for silicone oil immersion. Supplementary file 2 contains the measured structural data of the manufactured system from Supplementary file 1. Supplementary files 3-5 contain the measured structural data of the manufactured systems after iterative surface shape correction for diffraction limited focusing in water-, silicone-, and high-RI oil immersion. Wave optical validation used a simulation model derived from the ray optical design files as previously reported[57], and applied the Fast Polarized Wave Propagation Method (FPWPM)[31] with a sampling step size of $\lambda/5$. As boundaries for diffraction limited performance, we considered the Airy disk diameter in the lateral- and twice the Rayleigh length in the axial dimension.

Manufacturing

The optical surfaces were exported to a computer aided design (CAD) file and compiled to a 3D-printing model together with mechanical supports and microfluidic vias for encapsulation, using the CAD software Solidworks (Dassault Systèmes, Vélizy-Villacoublay, France). The single mode fibers (780HP, Thorlabs, Newton, New Jersey, USA) and the 650 µm long coreless fused silica fiber pieces (FG125LA, Thorlabs, Newton, New Jersey, USA) were spliced with a Vytran GPX3800 automated glass processor (Thorlabs, Newton, New Jersey, USA). The three 3D-PRIMOPS variants were manufactured with a commercially available femtosecond 3D-printer (Photonic Professionl GT2) from proprietary IP-S photoresist (both Nanoscribe GmbH, Eggenstein-Leopoldshausen, Germany) using a 40x/1.4 objective lens (Plan-Apochromat 40x/1.4 Oil DIC M27, Zeiss, Oberkochen, Germany). The 3D-PRIMOPS lenses were developed in Propylenglycolmonomethyletheracetate (PGMEA) for 3 h and then rinsed with isopropanol (both Merck KGaA, Darmstadt, Germany) for 2 min.

For microfluidic sealing, we used the same IP-S photoresist to fill the microfluidic channels under a microscope setup. In preliminary experiments, we determined channels with 12.5 µm width and vias with quadratic cross-sections and 10 µm side-length to retain the liquid IP-S reliably. The liquid IP-S inside the channels was cured with a UV lamp (UV-Power Pen 2.0, Hoenle AG, Gilching, Germany).

Experimental quantification of point spread functions

The 3D-PRIMOPS was directly dipped into the immersion medium (deionized water: n = 1.33, silicone: n = 1.4, immersion oil: n = 1.52, Immersol 518 F, Carl Zeiss AG, Oberkochen, Germany), and illuminated with a $\lambda = 782.5$ nm laser source (S1FC785, Thorlabs, Newton, New Jersey, USA). The projected focal spot was imaged with a video microscope, using a macroscopic immersion objective lens (LD LCI Plan-Apochromat 40x/1.2 Imm Korr DIC M27, Carl Zeiss AG, Oberkochen, Germany). A piezoelectric stepper (PIFOC P-725.1, Physik Instrumente GmbH, Karlsruhe, Germany) scanned the objective lens along the optical axis, with a step size of $\Delta z = 0.12$ µm, to obtain volume image stacks of the focal spot.

Acknowledgements

We acknowledge funding from: Carl-Zeiss-Stiftung (EndoPrint3D); University of Stuttgart (RiSC); Federal Ministry of Education and Research (GeDeSens2Virus, Project 16ME0374); The Baden-Württemberg Stiftung (Elite Programme for Postdocs). Marco Wende is supported by a Joachim Herz Foundation Add-on Fellowship. We thank Alois M. Herkommer and Harald Giessen for fruitful discussion and access to facilities at their institutes, and Pavel Ruchka for technical assistance with fiber splicing. We thank Andreas Boes and Rouven Klenk for insightful discussions on applications in the field of PICs. We acknowledge DESY (Hamburg, Germany), a member of the Helmholtz Association HGF, for provision of experimental facilities. Parts of this research were carried out at Petra III and we thank Fabian Wilde for assistance with X-ray microtomography. Beamtime was allocated for proposal I-20231354 at beamline P05. We thank Florian Hiering, Jule Grunewald, and Oliver Walker for their support during beamtime measurements.

Author details
[1]Institute of Applied Optics (ITO), University of Stuttgart, Pfaffenwaldring 9, 70569 Stuttgart, Germany. [2]Research Center SCoPE, University of Stuttgart, Pfaffenwaldring 57, 70569 Stuttgart, Germany. [3]Institute of Biomaterials and Biomolecular Systems, University of Stuttgart, Pfaffenwaldring 57, 70569 Stuttgart

Data availability
Data underlying the results presented in this paper are not publicly available at this time but may be obtained from the authors upon reasonable request.

Conflict of interest
The authors declare no conflicts of interest.

Received: 19 June 2024 Revised: 17 January 2025 Accepted: 18 January 2025
Accepted article preview online: 24 February 2025

References

1. Dhawan, A. P., D' Alessandro, B. & Fu, X. L. Optical imaging modalities for biomedical applications. *IEEE Reviews in Biomedical Engineering* **3**, 69-92 (2010).
2. Keiser, G. et al. Review of diverse optical fibers used in biomedical research and clinical practice. *Journal of Biomedical Optics* **19**, 080902 (2014).
3. Kotnala, A. et al. Microfluidic-based high-throughput optical trapping of nanoparticles. *Lab on a Chip* **17**, 2125-2134 (2017).
4. Heuer, C. et al. 3D printing in biotechnology- an insight into miniaturized and microfluidic systems for applications from cell culture to bioanalytics. *Engineering in Life Sciences* **22**, 744-759 (2022).
5. Yang, Z. Y. et al. Miniaturization of optical spectrometers. *Science* **371**, eabe0722 (2021).
6. Gonzalez-Hernandez, D. et al. Micro-optics 3D printed via multi-photon laser lithography. *Advanced Optical Materials* **11**, 2201701 (2023).
7. Gissibl, T. et al. Two-photon direct laser writing of ultracompact multi-lens objectives. *Nature Photonics* **10**, 554-560 (2016).
8. Toulouse, A. et al. 3D-printed miniature spectrometer for the visible range with a 100×100 μm^2 footprint. *Light: Advanced Manufacturing* **2**, 20-30 (2021).
9. Malinauskas, M. et al. Femtosecond laser polymerization of hybrid/integrated micro-optical elements and their characterization. *Journal of Optics* **12**, 124010 (2010).
10. Kampmann, R., Sinzinger, S. & Korvink, J. G. Optical tweezers for trapping in a microfluidic environment. *Applied Optics* **57**, 5733-5742 (2018).
11. Pallaoro, A. et al. Rapid identification by surface-enhanced raman spectroscopy of cancer cells at low concentrations flowing in a microfluidic channel. *ACS Nano* **9**, 4328-4336 (2015).
12. Kong, K. et al. Raman spectroscopy for medical diagnostics—from in-vitro biofluid assays to in-vivo cancer detection. *Advanced Drug Delivery Reviews* **89**, 121-134 (2015).
13. Cordero, E. et al. In-vivo raman spectroscopy: from basics to applications. *Journal of Biomedical Optics* **23**, 071210 (2018).
14. Kim, S. A., Heinze, K. G. & Schwille, P. Fluorescence correlation spectroscopy in living cells. *Nature Methods* **4**, 963-973 (2007).
15. Yu, L. et al. A comprehensive review of fluorescence correlation spectroscopy. *Frontiers in Physics* **9**, 644450 (2021).
16. Miller, D. A. B. Device requirements for optical interconnects to silicon chips. *Proceedings of the IEEE* **97**, 1166-1185 (2009).
17. Lindenmann, N. et al. Photonic wire bonding: a novel concept for chip-scale interconnects. *Optics express* **20**, 17667-17677 (2012).
18. Lindenmann, N. et al. Connecting silicon photonic circuits to multicore fibers by photonic wire bonding. *Journal of lightwave Technology* **33**, 755-760 (2015).
19. Marchetti, R. et al. Coupling strategies for silicon photonics integrated chips[Invited]. *Photonics Research* **7**, 201-239 (2019).
20. Mu, X. et al. Edge couplers in silicon photonic integrated circuits: A review. *Applied Sciences* **10**, 1538 (2020).
21. Dietrich, P. I. et al. In situ 3D nanoprinting of free-form coupling elements for hybrid photonic integration. *Nature Photonics* **12**, 241-247 (2018).
22. aaaTrappen, M. et alaa. 3D-printed optical probes for wafer-level testing of photonic integrated circuits. *Optics Express* **28**, 37996-38007 (2020).
23. Bremer, L. et al. Quantum dot single-photon emission coupled into single-mode fibers with 3D printed micro-objectives. *APL Photonics* **5**, 106101 (2020).
24. Sartison, M. et al. 3D printed micro-optics for quantum technology: Optimised coupling of single quantum dot emission into a single-mode fibre. *Light: Advanced Manufacturing* **2**, 103-119 (2021).
25. Plidschun, M. et al. Ultrahigh numerical aperture meta-fibre for flexible optical trapping. *Light: Science & Applications* **10**, 57 (2021).
26. Asadollahbaik, A. et al. Fresnel lens optical fiber tweezers to evaluate the vitality of single algae cells. *Optics Letters* **47**, 170-173 (2022).
27. Asadollahbaik, A. et al. Highly efficient dual-fiber optical trapping with 3D printed diffractive fresnel lenses. *ACS Photonics* **7**, 88-97 (2020).
28. Varapnickas, S. et al. Birefringent optical retarders from laser 3D-printed dielectric metasurfaces. *Applied Physics Letters* **118**, 151104 (2021).
29. Vanmol, K. et al. Fabrication of multilevel metalenses using multiphoton lithography: from design to evaluation. *Optics Express* **32**, 10190-10203 (2024).
30. Noponen, E., Turunen, J. & Vasara, A. Electromagnetic theory and design of diffractive-lens arrays. *Journal of the Optical Society of America A* **10**, 434-443 (1993).
31. Wende, M. et al. Fast algorithm for the simulation of 3D-printed microoptics based on the vector wave propagation method. *Optics Express* **30**, 40161-40173 (2022).
32. Ovsianikov, A. et al. Ultra-low shrinkage hybrid photosensitive material for two-photon polymerization microfabrication. *ACS Nano* **2**, 2257-2262 (2008).
33. KayakuAM. SU-8 photoresist. (2024). at https://kayakuam.com/products/su-8-photoresists/ URL.
34. Malinauskas, M. et al. 3D microoptical elements formed in a photostructurable germanium silicate by direct laser writing. *Optics and Lasers in Engineering* **50**, 1785-1788 (2012).
35. Gissibl, T. et al. Refractive index measurements of photo-resists for three-dimensional direct laser writing. *Optical Materials Express* **7**, 2293-2298 (2017).
36. Schmid, M., Ludescher, D. & Giessen, H. Optical properties of photoresists for femtosecond 3D printing: refractive index, extinction, luminescence-dose dependence, aging, heat treatment and comparison between 1-photon and 2-photon exposure. *Optical Materials Express* **9**, 4564-4577 (2019).
37. Weber, K. et al. Tailored nanocomposites for 3D printed micro-optics. *Optical Materials Express* **10**, 2345-2355 (2020).
38. Lü, C. L. & Yang, B. High refractive index organic–inorganic nanocomposites: design, synthesis and application. *Journal of*

Materials Chemistry **19**, 2884-2901 (2009).
39. Tao, P. et al. TiO_2 nanocomposites with high refractive index and transparency. *Journal of Materials Chemistry* **21**, 18623-18629 (2011).
40. Werdehausen, D. et al. Design rules for customizable optical materials based on nanocomposites. *Optical Materials Express* **8**, 3456-3469 (2018).
41. Werdehausen, D. et al. Dispersion-engineered nanocomposites enable achromatic diffractive optical elements. *Optica* **6**, 1031-1038 (2019).
42. Gross, H. Handbook of Optical Systems Volume 1: Fundamentals of Technical Optics (Weinheim: WILEY-VHC, 2005).
43. Zyla, G. et al. 3D micro-devices for enhancing the lateral resolution in optical microscopy. *Light: Advanced Manufacturing* **5**, 204-217 (2024).
44. Kirchner, R., Chidambaram, N. & Schift, H. Benchmarking surface selective vacuum ultraviolet and thermal postprocessing of thermoplastics for ultrasmooth 3-D-printed micro-optics. *Optical Engineering* **57**, 041403 (2018).
45. Rothermel, F. et al. Fabrication and characterization of a magnetic 3D-printed microactuator. *Advanced Materials Technologies* **9**, 2302196 (2024).
46. Stein, O. et al. Fabrication of low-density shock-propagation targets using two-photon polymerization. *Fusion Science and Technology* **73**, 153-165 (2018).
47. Williams, H. E. et al. Fabrication of three-dimensional micro-photonic structures on the tip of optical fibers using SU-8. *Optics express* **19**, 22910-22922 (2011).
48. Liao, C. Z., Wuethrich, A. & Trau, M. A material odyssey for 3D nano/microstructures: two photon polymerization based nanolithography in bioapplications. *Applied Materials Today* **19**, 100635 (2020).
49. Toulouse, A. et al. Ultra-compact 3D-printed wide-angle cameras realized by multi-aperture freeform optical design. *Optics Express* **30**, 707-720 (2022).
50. Weinacker, J. et al. On iterative pre-compensation of 3D laser-printed micro-optical components using confocal-optical microscopy. *Advanced Functional Materials* **34**, 2309356 (2024).
51. Galvez, D. et al. Characterizing close-focus lenses for microendoscopy. *Journal of Optical Microsystems* **3**, 011003 (2023).
52. Li, J. W. et al. 3D-printed micro lens-in-lens for in vivo multimodal microendoscopy. *Small* **18**, 2107032 (2022).
53. Toulouse, A. et al. Alignment-free integration of apertures and nontransparent hulls into 3D-printed micro-optics. *Optics Letters* **43**, 5283-5286 (2018).
54. Wilde, F. et al. Micro-CT at the imaging beamline P05 at PETRA III. *AIP conference Proceedings* **1741**, 030035 (2016).
55. Bianchi, S. et al. Focusing and imaging with increased numerical apertures through multimode fibers with micro-fabricated optics. *Optics letters* **38**, 4935-4938 (2013).
56. Doth, K., Haist, T. & Reichelt, S. Towards pathogen detection with 3D-printed micro-optics in microfluidic systems. Proceedings of SPIE 12876, Laser 3D Manufacturing XI. San Francisco, California, United States: SPIE, 2024, 172-175.
57. Drozella, J. et al. Fast and comfortable GPU-accelerated wave-optical simulation for imaging properties and design of highly aspheric 3D-printed freeform microlens systems. Proceedings of SPIE 11105, Novel Optical Systems, Methods, and Applications XXII. San Diego, California, United States: SPIE, 2019, 27-33.